California Polytechnic State University
San Luis Obispo

Department of Physics

Correlations in Intensity Fluctuations From a Quasi-Thermal Light Source: An Application of Hanbury Brown & Twiss

A Senior Project Presented in Partial Fulfillment of the Requirements for the Degree
Bachelor of Science, Physics

By:
Christopher Watanabe

Supervised By:
Dr. John Sharpe

Submitted: March 20, 2015

Correlations in Intensity Fluctuations From a Quasi-Thermal Light Source: An Application of Hanbury Brown & Twiss

Christopher R. Watanabe
California Polytechnic State University
Senior Project

In this experiment, the observation by Hanbury Brown and Twiss that light intensity fluctuations from an extended broadband source are spatially correlated is demonstrated with a quasi-thermal light source. Laser light is used to illuminate a ground glass screen and generate a diffraction pattern, also known as a speckle pattern. The speckle pattern is recorded using an electronic camera and analyzed. Calculated auto-correlations of the intensity fluctuations agree with theoretical results originating from speckle analysis.

I. Introduction

Hanbury Brown and Twiss (HBT) demonstrated in 1958 [1] that scattered light collected from an extended source is partially correlated. An outline of their experimental setup is shown in Fig. 1. Light from a filtered mercury lamp was incident on a small aperture (the aperture thus became the light source) and propagated through free space to the detectors where the light intensity was converted to a current using photomultiplier tubes. These photocurrent signals were then processed and correlated together; the correlation measured as a function of the separation between the detectors. HBT found that the intensity fluctuations had a spatial dependence - that the fluctuations were strongly correlated when the detectors were close together and less so when the detectors were further apart. The spatial extent of the correlation depended on the aperture size, the distance from the source to the detectors, and the wavelength of the light. Based on these early experiments HBT went on to use this technique to measure the apparent size of the star Sirius [2].

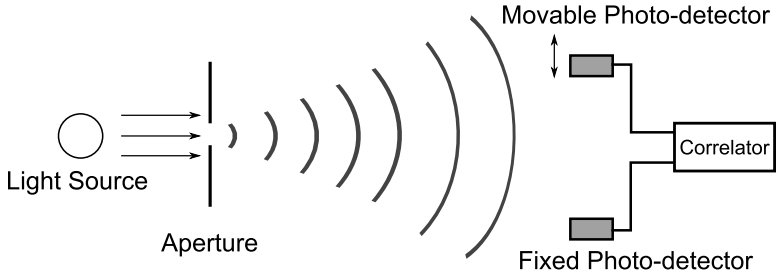

Figure 1: HBT's setup to measure intensity correlations.

While the general theory of the observations of HBT is quite involved, a feeling for the origin of the effect can be gained by considering a very simple source configuration where the emitting object is composed of just two independent point sources, each emitting just two wavelengths of light [5]. Furthermore, the source is placed a great distance from the detectors so that the light arriving at the detectors is essentially in the form of plane waves, but with the waves slightly tilted with respect to each other. The situation is sketched in Fig. 2.

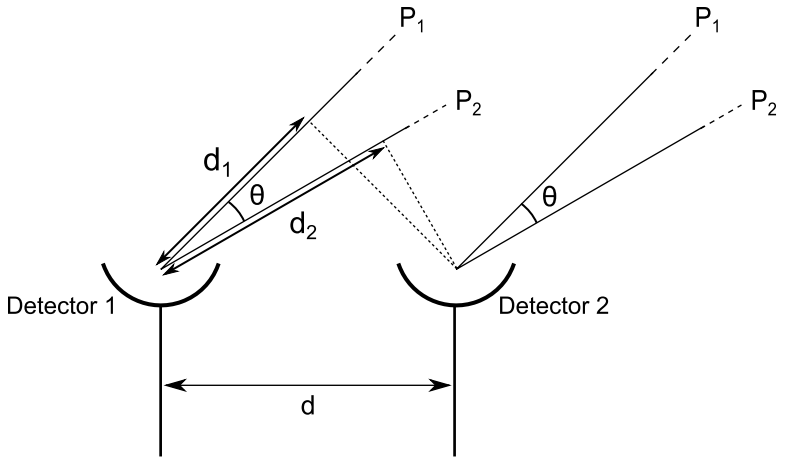

Figure 2: A simple configuration of two independent point sources composed of two wavelengths incident upon two photo-detectors. As shown, light from sources P_1 & P_2 must travel an additional distance d_1 and d_2, respectively, to reach detector 1. As shown by HBT, the signals observed at the two detectors are correlated temporally, as a function of the separation distance d.

Beginning with a basic two beam system consisting of two frequencies originating from a distant, extended source, one can show that a correlation between arriving waves exists. The incident electric fields are given by

$$E_1 sin(\omega_1 t + \phi_1) \qquad E_2 sin(\omega_2 t + \phi_2) \tag{1}$$

The intensity measured at one detector is proportional to the square of the total E-field

$$I_1 = (E_1 sin(\omega_1 t + \phi_1) + E_2 sin(\omega_2 t + \phi_2))^2$$

Similarly, if we look at the intensity at a second detector, we observe a similar result, but modified due to the difference in optical path length caused by the detector separation distance (see Fig. 2)

$$I_2 = (E_1 sin(\omega_1 (t + d_1/c) + \phi_1) + E_2 sin(\omega_2 (t + d_2/c) + \phi_2))^2$$

Expanding the intensity values above shows that the resultant intensity functions contain a more complex band of frequencies than were contained in the incident fields upon the detectors. Using a low-pass filter, it is possible to limit the observed intensity frequency to $\omega_1 - \omega_2$, which then simplifies the respective intensity functions to

$$I_1 = E_1 E_2 cos((\omega_1 - \omega_2)t + (\phi_1 - \phi_2))$$
$$I_2 = E_1 E_2 cos((\omega_1 - \omega_2)t + (\phi_1 - \phi_2) + (\omega_1 d_1 - \omega_2 d_2)/c)$$

In correlating these intensity functions, that is multiplying and time-averaging, we obtain the following correlation function

$$\langle I_1(t)I_2(t)\rangle = E_1^2E_2^2cos[(\omega/c)(d_1 - d_2)] \tag{2}$$

which is the expected correlation for *one* filtered frequency (letting $\omega_1 = \omega_2 = \omega$) of the many that are represented in the intensity functions. In order to analyze the intensity functions completely, it would be necessary to integrate over all represented frequencies, as well as integrate over the entire, extended source. However, this single result is enough to demonstrate that intensity variations at the observation plane are indeed correlated, as will be shown in this experiment.

That this result could also pertain to light of low intensity - so low that the quantized nature of the detection has to be taken into account - came as a surprise to many supporters of the growing theory of quantum mechanics, as they believed these results violated the uncertainty principle. This was particularly caused by viewing HBT's research in terms of the particle nature of light; for photons emitted randomly from a thermal source, how was it that they could possibly have correlated arrival times at two detectors, i.e. be detected pair-wise. In one sense, HBT set the stage for further investigation into the nature of light/matter interaction and quantum effects. For the rest of this work however, classical wave optics suffices.

The original experiment undertaken by HBT is, to this day, quite challenging. This is because light from a thermal source (the mercury lamp) is not very bright and, even though they used only one spectral line from the source, the bandwidth is large enough to create extremely rapid fluctuations in intensity. From an experimental point of view, these problems were alleviated by the invention of the quasi-thermal light source in 1964 by Martienssen and Spiller (MS) [4]. This is done by taking a laser beam and illuminating a moving ground glass screen, which results in scattering.

One way of thinking about the scattered light is as follows: randomly diffracted light receives a Doppler shift due to the movement of the screen, which generates a narrow band of frequencies about the laser frequency. Since the shifts are fairly small for slowly moving scatterers, the temporal rate of fluctuation of the intensities is also low, typically on the order of kHz. That being said, there is an alternative and equally valid way of looking at the light scattering process. We first recognize that the scattered light from a fixed ground glass screen leads to a speckle pattern due to the random interference of the scattered light. When the screen is now set in motion the random scatterers are gradually replaced by another random set which causes the interference pattern to evolve and change. Using this as their light source, in an arrangement similar to HBT's experimental setup, Martiensson and Spiller collected the light fluctuations using two photo-detectors separated by a variable distance, d (see Fig. 2).

As with HBT, this experiment led to the same conclusion, scattered light fluctuations are partially correlated over the observation plane. MS particularly stressed HBT's links between the coherence of two light beams, or their fixed interference field, to the correlations of their intensity fluctuations - namely that two beams are coherent if their fluctuations are correlated. This is shown in their experimental data/analysis shown in Fig. 3.

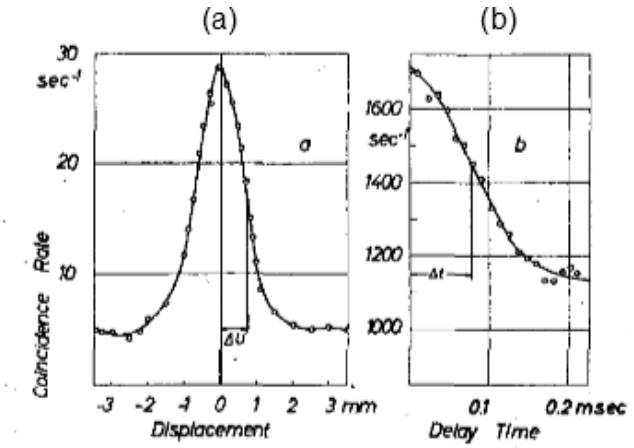

Figure 3: a: Martiensson & Spiller's experimental measurements of photon coincidence rates (a measure of correlation) as a function of the displacement distance between detectors. b: Measured coincidence rates as a function of temporal delay. [4]

This project is a combination of the aforementioned experiments. We take the basic idea of HBT, and rather than look at the temporal correlations of the signals as we move the detectors, we collect the light all at once using an electronic camera. While we could then proceed to look at the temporal correlations of the light between different pixels of the detector as the light field evolves, we choose instead to look at the spatial correlations of the light intensity for a fixed field. It seems reasonable that the correlations in each case should be the same. This experiment demonstrates that they are.

II. Experimental Design

As discussed above, when coherent light strikes irregularities on the surface of an object, it is scattered at different angles, producing a diffraction pattern at the observation plane known as speckle. If the object is put into motion, it produces a dynamic interference pattern through a process called Dynamic Light Scattering (DLS), as demonstrated in Fig. 4.

In this experiment, a ground glass screen is used to scatter coherent light from a 532 nm laser, the speckle pattern of which is shown in Fig. 6(b). The scattered light is subsequently passed through a slit, which serves to diffract and widen the speckle pattern produced by DLS. The diffraction pattern is then observed at the far field with a converging lens and collected by a two dimensional, area scan camera (Basler pilot: model piA2400 - 17gm) controlled by the Pylon Application Programming Interface (API) software. The experimental setup is shown in Fig. 5.

The API software controlling the Basler camera allows the user to control specific characteristics of the camera, including the frame rate, shutter speed, and gain. Each measurement taken with the camera consisted of 10 frames, taken at a shutter speed of 80μs and a frame rate of 5 frames per second. While the camera is capable of 100+ frames per second, it is important to allow the speckle pattern to evolve between frames in order to ensure that each frame is independent of the next. This allows us to collect several fixed speckle patterns. For more detail on the use of the Pylon software, see Appendix A.

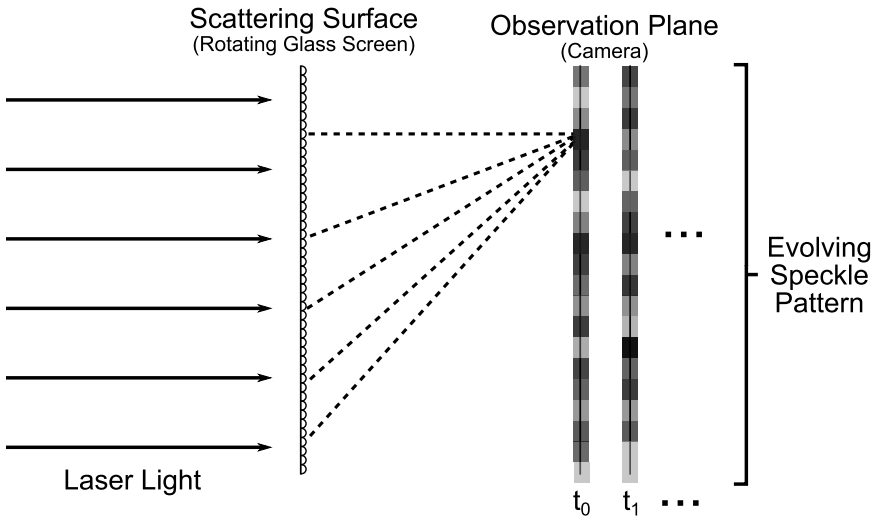

Figure 4: Dynamic light scattering occurs when light strikes inhomogeneities on the surface of a moving object. The constructive and destructive interference of DLS generates a speckle pattern that evolves with time.

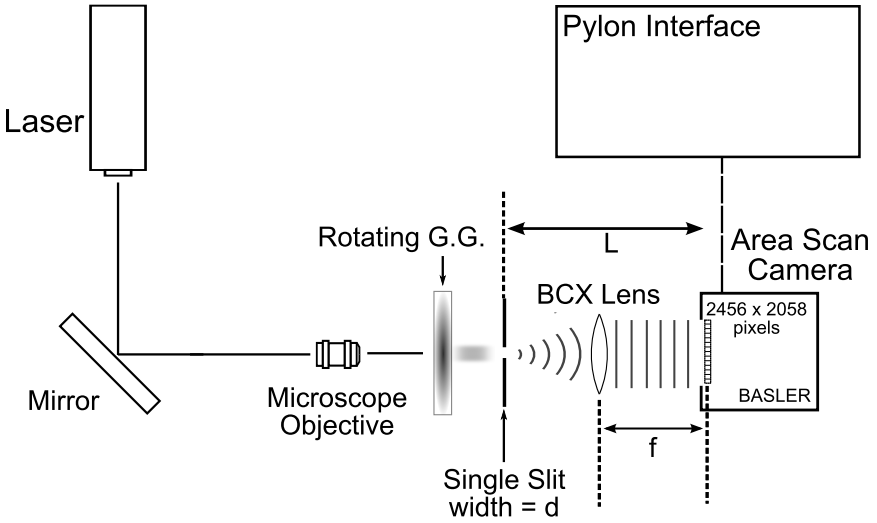

Figure 5: Light from a 532 nm laser is focused upon a ground glass screen with a microscope objective. The produced speckle pattern is passed through a single slit and focused at "infinity" using a bi-convex lens. The speckle pattern is captured with a 2D Basler area scan camera and viewed with the Pylon Interface Software.

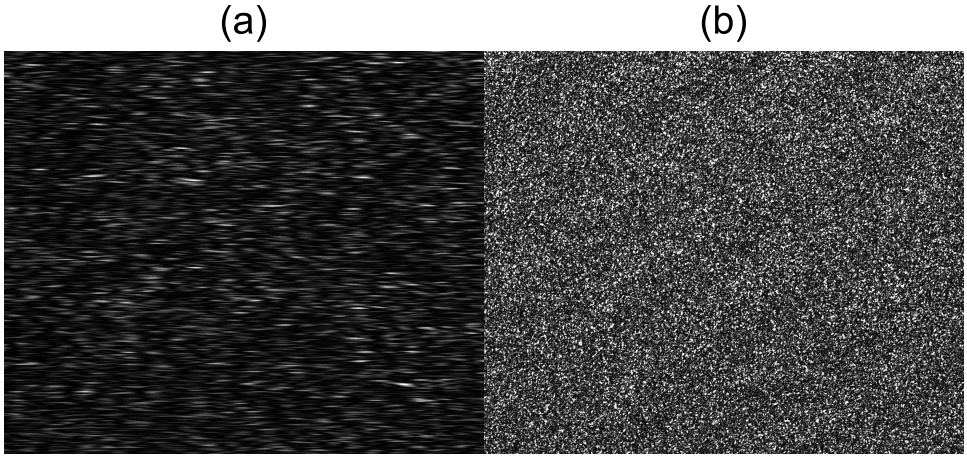

Figure 6: A comparison of speckle with the slit (a) and without the slit in place (b).

The use of a thin slit increases the width of the speckle pattern from DLS, as shown in Fig. 6. This broadening is well known for physical optics, where the angular width of the diffraction pattern, theta, taken as the distance from the center of the pattern to the 1st minimum, is given by

$$asin(\theta) = \lambda \tag{3}$$

where a is the slit width, theta is the angular width of diffraction and λ is the wavelength of incident light. Points within the slit act as spherical wave front sources, thereby producing a diffraction pattern at the observation plane. The converging lens that follows the slit focuses the speckle pattern at the focal point of the lens, essentially turning the spherical wave fronts into planar waves, and thus locating the observation field at "infinity".

After collecting the data with the camera at the observation plane, each horizontal line of each frame is auto-correlated using the xcorr function of MATLAB. Before any correlation is calculated however, the mean value of the frame is subtracted from each pixel. We found that the use of a three point smoothing function reduced electronic noise and yielded a smoother auto-correlation function at the zeroeth lag. The smoothed frames are then separated into rows, which are then auto-correlated and averaged to give the auto-correlation function of the entire frame. Once frame correlations are calculated for each of the 10 frames taken, they are averaged to give the final auto-correlation. The auto-correlation process is shown in detail in Fig. 7, and the MATLAB script is given in Appendix B.

Theory [3] predicts the following form for the auto-correlation function:

$$C(u) = \left| sinc\left(\frac{\pi u d}{\lambda L}\right)\right|^2 \tag{4}$$

where u is the pixel distance, d is the width of the slit, λ is the wavelength of scattered light, L is the separation distance between the slit and pixel array, and the sinc function is defined as sinc(x) = sin(x) / x. By comparing experimentally measured auto-correlations at various slit widths to theory, we demonstrate that intensity functions measured over the 2D array are indeed spatially correlated.

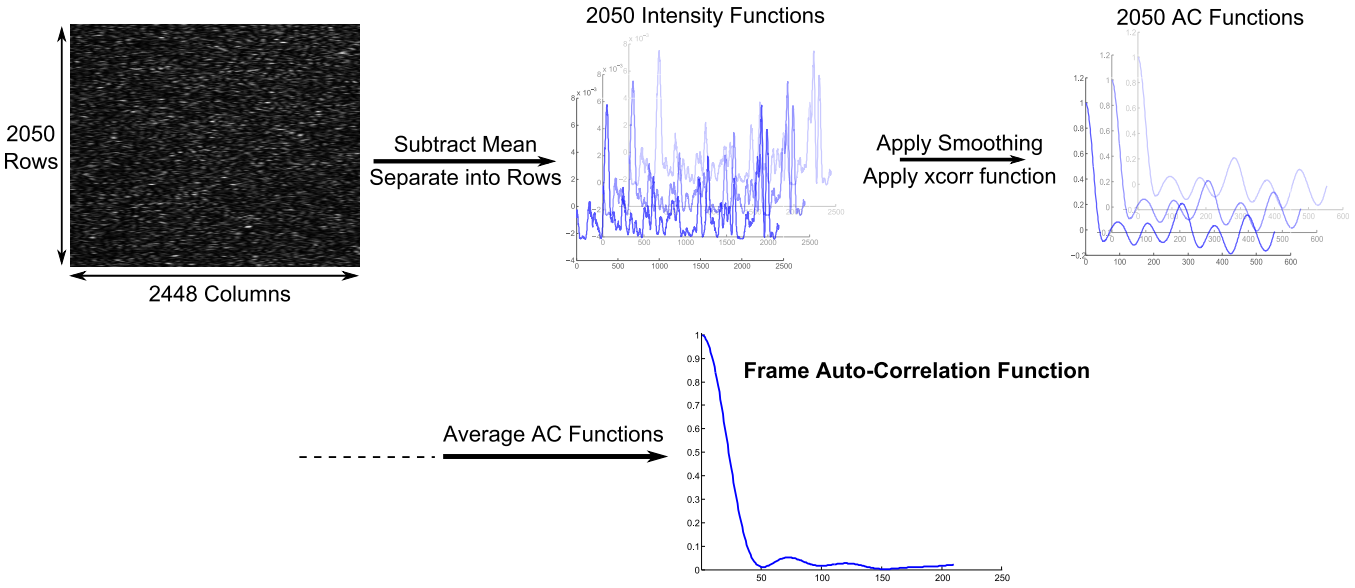

Figure 7: The auto-correlation (AC) process for one frame. This is done for each of 10 frames that are taken at a given slit width. The 10 frame correlations are then averaged to yield an overall auto-correlation for the slit width.

III. Analysis

Measured and theoretical correlations for slit widths of 400μm, 600μm, and 800μm are shown in Fig.s 8, 9, and 10. Measured correlations closely follow the theoretical sinc^2 form.

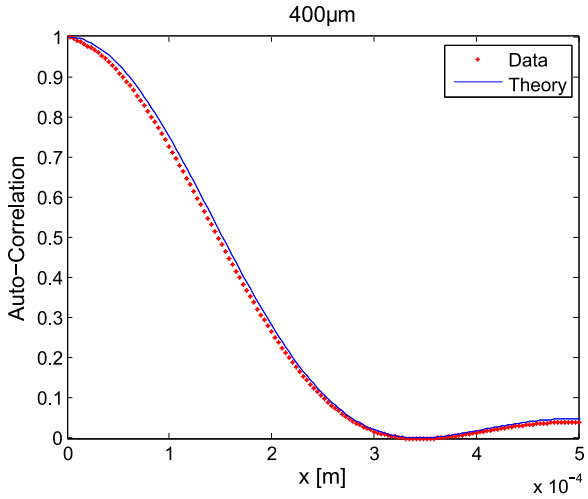

Figure 8: Measured and theoretical correlations for a 400μm slit width.

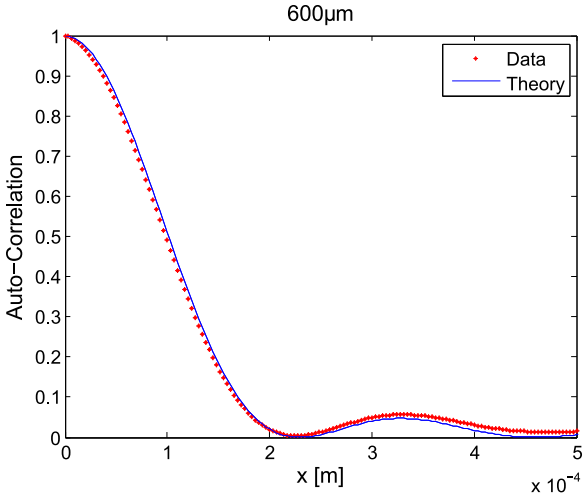

Figure 9: Measured and theoretical correlations for a 600μm slit width.

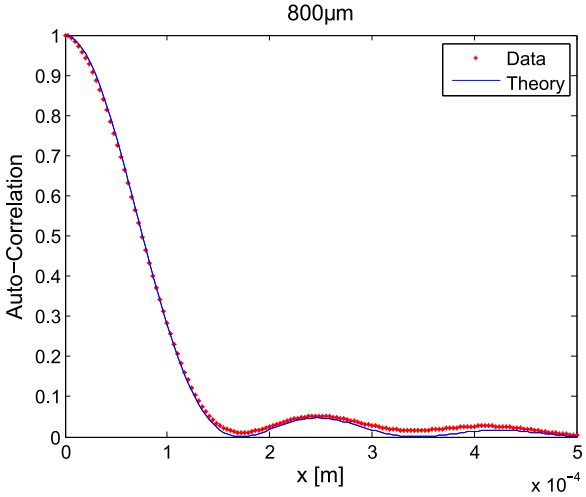

Figure 10: Measured and theoretical correlations for a 800μm slit width.

IV. Conclusion

In this experiment, Hanbury Brown and Twiss' observation that light intensity functions from DLS are partially correlated at the observation plane was demonstrated by spatially correlating fixed interference fields collected from DLS from a ground glass screen. Measured auto-correlations of the intensity fluctuations at various slit sizes agreed with results originating from theory. From this we conclude that spatial correlations over the observation plane follow the same pattern that is expected from temporal correlations as a function of the detector separation distance.

References

[1] R. Hanbury Brown, R. Twiss
Interferometry of the Intensity Fluctuations in Light. II. An Experimental Test of the Theory for Partially Coherent Light., Proc. R. Soc. Lond. A, **243**, pp. 291-319 (1958)

[2] R. Hanbury Brown, R. Twiss
Interferometry of the Intensity Fluctuations in Light. IV. A Test of an Intensity Interferometer on Sirius A, Proc. R. Soc. Lond. A, **248**, pp. 222-237 (1958)

[3] Joseph W. Goodman
Speckle Phenomena in Optics: Theory and Applications, Roberts & Company, Greenwood Village, CO (2007)

[4] W. Martiennsen, E. Spiller
Coherence and Fluctuations in Light Beams, American Journal of Physics, **32**, pp. 919-926 (1964)

[5] Mark. P. Silverman
More than One Mystery: Explorations in Quantum Interference, Springer-Verlag New York, Inc., New York, NY, pp. 59-63 (1995)

Appendix A: Using the Pylon API Software

The Pylon Application Programming Interface is shown in Fig. 11. As can be seen, the interface consists of a visual display of the connected camera and zoom/record/freeze frame capabilities. It gives the user the ability to set many settings on the camera, including the gain, shutter speed, and frame rate, as demonstrated in Fig. 11 and 12.

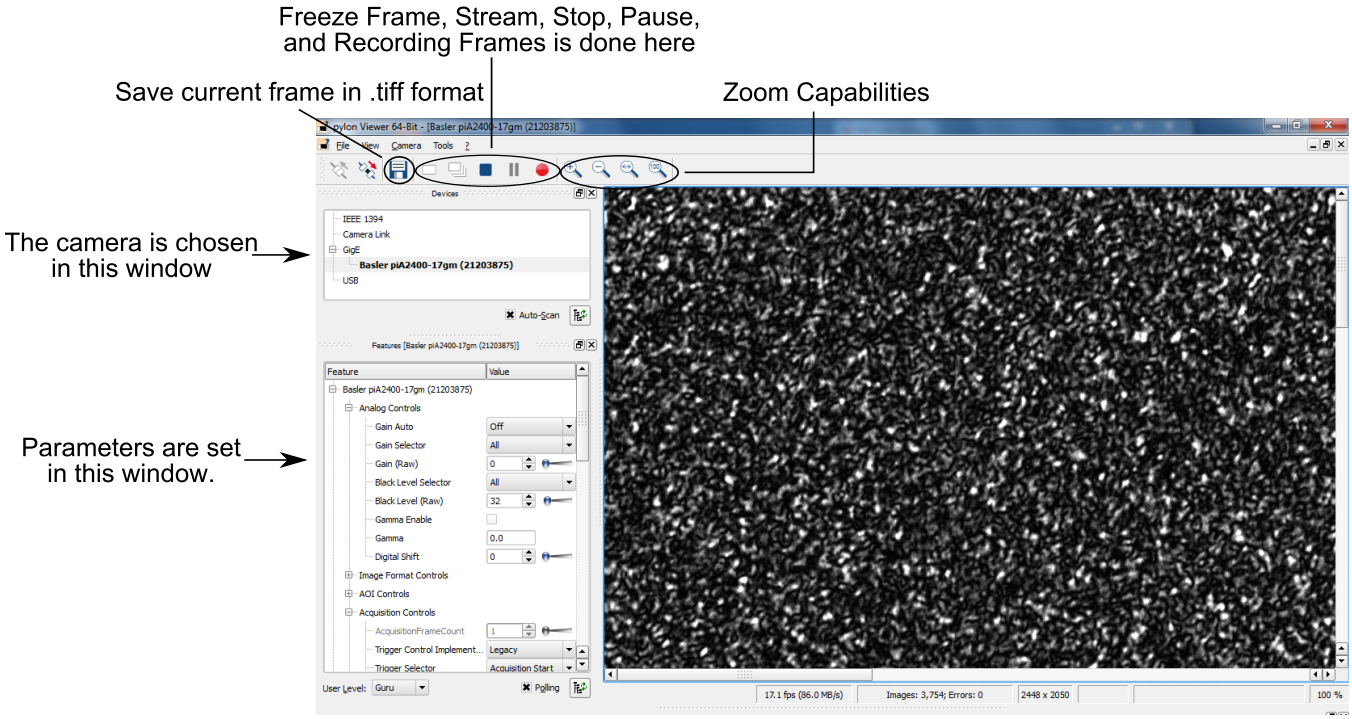

Figure 11: A snapshot of the Pylon API used to gather experimental data via communication with an electronic camera.

To control the saturation of the intensity fluctuations measured with the camera, the Pylon software enables the user to control the gain of the camera. In the case that a minimum/maximum gain yields undesirable measurements, the intensity can be further modified by changing the amplification of the laser.

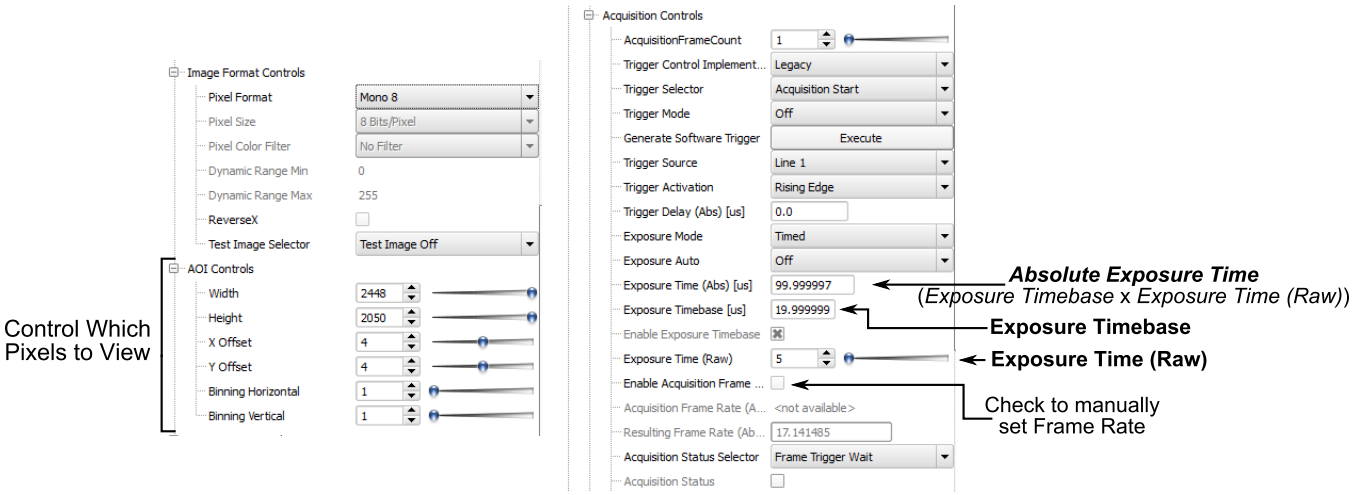

Figure 12: Camera controls via the API include shutter speed, frame rate, exposure time, and direct control over which pixels of the camera to communicate with.

There are two ways to set the exposure time of the camera. Using the control *Exposure Time (Abs) [µs]*, the desired exposure time can be entered. It is also possible to set the exposure time by setting the desired *Exposure Timebase [µs]* and the *Exposure Time (Raw)*. While the practicality of such a method is unclear, the *Exposure Time (Abs)* = *Exposure Timebase [µs]* x *Exposure Time (Raw)*.

Appendix B: MATLAB Code for Auto-Correlation

- Convert Frames From an AVI Into an Array of Intensity Values, and Auto-Correlate these Arrays by row.
- Create Theoretical Curves Based on the Sinc Function, and plot with experimental data points to verify experimental data agrees with theory.

%% Convert Frames From an AVI Into an Array of Intensity Values, and Auto-Correlate these Arrays by row.

```
clear all
close all

% Read in AVIs for each slit size, containing 10 frames, into the MATLAB workspace.

myFolder = pwd;
filePattern = fullfile(myFolder, '*.avi');
aviFiles = dir(filePattern);

for i = 1:length(aviFiles)

    baseFileName = aviFiles(i).name;
    number(i) = str2num(strrep(baseFileName, 'um.avi', ''));
    fullFileName = fullfile(myFolder, baseFileName);
    mov = aviread(fullFileName);

    % Separate the frames and turn them into data arrays based on pixel.

    for j = 2:length(mov)

        % Convert frame to an array of numerical values.

        frame = double(frame2im(mov(j)));
        h = size(frame,1);
        w = size(frame,2);
        x = 0:2448;

        % Subtract the mean of the frame from the frame.
        % Mean and sum twice: Once for mean of the columns, once for mean
        % of rows.

        frame = frame - mean(mean(frame));
        M = sum(sum(frame.*frame)) / (640*480);
        frame = frame/M;
```

```
        % Apply smoothing function to each row and auto-correlate.

        for k = 1:h

             line = smooth(frame(k,:));
             lineCorr(k,:) = xcorr(line, 'coeff');

        end

        % Take the mean of the row auto-correlations to calculate the
        % frame's auto-correlation function.

         frameCorr(j-1,:) = mean(lineCorr);

    end

    % Reindex.

     totalCorr(i,:) = frameCorr(i,:);

end
```

%% Create Theoretical Curves Based on the Sinc Function, and plot with experimental data points to verify experimental data agrees with theory.

```
% Sort the Experimental Auto-Correlations by Slit Width.

num = sort(number);

for n = 1:length(num)
    index = find(num(n) == number);
    tCorr(n,:) = totalCorr(index,:);
end

% Set Parameters for Slit Width, Pixel Number, Wavelength, and Separation
% Distance.

d = num * 1E-6;
u = (0:640) * 3.45E-6;
lambda = 532E-9;
L = 0.26;

% Generate Theoretical Curves.
```

```
for i = 1:length(d)

   tCurve(i,:) = sinc(u*d(i)/lambda/L).^2;

end

% Plot the Experimental & Theoretical Auto-Correlation for each slit width.

for i = 1:length(num)

    figure(i)
    plot(u(1:210), tCorr(i,2448:2657), 'r*', 'MarkerSize', 3)
    xlim([0 0.0005])
    hold on
    plot(u(1:210), tCurve(i,1:210), 'b')
    plot(u(1:210), smooth(tCorr(i,2448:2657),3), 'g*', 'MarkerSize', 3)
    xlim([0 .0005])
    % plot(fittedmodel,'m')
    legend('Data', 'Theory')
    xlabel('x [m]', 'FontSize', 14)
    ylabel('Auto-Correlation', 'FontSize', 14)
    title(strcat(num2str(num(i)), 'um'), 'FontSize', 12)

end
```